Development of poly(lactic acid) cellular materials: Physical and morphological characterizations

J.-M. Julien [a,b,c], J.-C. Bénézet [c], E. Lafranche [a,b], J.-C. Quantin [c,*], A. Bergeret [c], M.-F. Lacrampe [a,b], P. Krawczak [a,b]

[a] Univ. Lille Nord de France, 59000 Lille, France
[b] Ecole des Mines de Douai, Department of Polymers and Composites Technology & Mechanical Engineering, 941 Rue Charles Bourseul, BP 10838, 59508 Douai, France
[c] Ecole des Mines d'Alès, Centre CMGD, 6 avenue de Clavières, 30319 Alès Cedex, France

A B S T R A C T

The present study aims at assessing the extrusion foaming characteristics of two commercial grades of poly(lactic acid) (PLA) using a chemical foaming agent (CFA). For each PLA the process was optimized based on a maximal void fraction criterion. The extruder die temperature significantly affects the void content (maximal for about 195 °C). An increase in the barrel temperature profile was also correlated with an increase in the void fraction. Moreover an increase in CFA concentration increased the PLA void fraction, and in some cases induced a decrease in cell density and an increase in cell size. Finally, an optimal value of 47% void fraction was obtained. Finally, optimally processed PLAs with varying CFA contents were tensile tested. The results pointed out that it was possible to observe significant decrease in the density and increase in some specific mechanical properties by controlling the extrusion foaming process.

Keywords:
Poly(lactic acid)
Extrusion foaming
Chemical foaming agent
Cell morphology

1. Introduction

In recent years sustainable development is a major priority. One way to overcome the issues related to the management of waste plastic parts, oil price fluctuations and the gradual depletion of fossil resources is to use polymers derived from renewable resources (bio-based polymers). Poly(lactic acid) (PLA) is a biodegradable polyester that can be used to alleviate the waste disposal problem. PLA generates both scientific and industrial interests [1–4], especially because of its mechanical properties which are equivalent or even superior to those of traditional polymers [5]. It is synthesized from L- and D-lactic acid, which are produced from the fermentation of sugar and polysaccharides such as sugar feedstocks and corn wheat with other starch sources, either by ring-opening polymerization or by condensation polymerization [1,6,7]. The biocompatibility and bioresorbability of PLA make it particularly well-suited for high value-added products (e.g. the medical field) [3,6,8]. Its ability to biodegradation [9] is also a major asset in the context of the development of plastic parts and plastics environmental impact (carbon footprint, life cycle optimization). Finally, it can be processed, without significant modifications by traditional plastic processing techniques for the production of films, fibres, extruded or injection moulded parts or foams and composite materials [6,10]. In view of reducing the environmental problems, replacement of traditional polymers with equivalent performance and weight reduction of the final product is also a subject of major industrial interest. Various solutions are currently the subject of special investigations, such as the substitution of certain constituents (replacing glass fibres with natural fibres) [11] or the manufacture of cellular products [12,13]. The latter method has an advantage of combining the weight reduction of the parts with potentially improved thermal and/or sound insulation properties.

In practice, polymer foams can be obtained by three main processes, one of them being the process used to obtain expanded polystyrene (EPS). The principle of this process is based on the production of expandable particles (0.2–3 mm in diameter), in which the polymer is heated to molten state in the presence of a foaming agent (such as pentane, hexane in general) or either by polymerization of styrene in presence of a foaming agent. The products obtained after moulding have a density typically in the range 10–30 kg/m^3. This process leads to rigid foams with closed cells. These foams find their application mainly in the packaging, construction, etc. [14,15]. Apart from EPS process, there are other techniques such as physical foaming and chemical foaming

* Corresponding author. Tel.: +33 (0)466785346; fax: +33 (0)466785365.
E-mail address: jean-christophe.quantin@mines-ales.fr (J.-C. Quantin).

processes. Physical foaming is achieved by injecting a gas (supercritical CO_2 or N_2) into the polymer matrix in order to obtain a micro-cellular structure with cell sizes around 10 microns with a cell density of 10^9 cells/cm^3. As concerns chemical foaming, it can be achieved with a solid additive (like chemical foaming agent so-called CFA) dispersed into the polymer matrix. With increase in temperature, CFA releases a gas, which is responsible for the foam formation. Further, CFAs are divided into two groups based on their enthalpy of reaction: the exothermic (azodicarbonamide which releases N_2 and other gases) and endothermic (sodium bicarbonate and citric acid which release CO_2 and H_2O) CFAs. These gases are responsible for a reduction in density of about 50% [14–16]. Today chemical foaming is the mostly used standard for the manufacture of cellular thermoplastic components. But nowadays, many novel foaming methods have been developed since conventional technologies by using combinations of physical foaming agent (CO_2) and alcohol (supercritical mixtures) [13], until specific and costly technologies which are based on the gas injection in an autoclave under pressure [5,17] or ice microparticles injection [18].

Finally, according to Greco et al. [21], the foam density depends on many processing parameters such as screw speed, die geometry, amount of CFA and processing temperature. Indeed, an increase in temperature leads to an increase in the density of foam. This is explained by the fact that the viscosity of the polymer decreases with increasing temperature. As a result, the polymer is unable to overcome the biaxial strain that occurs during cell growth, thus promoting coalescence or collapse of cells.

Although PLA is considered as a bio-sourced polymer with similar characteristics compared to conventional polymers, the fact remains that its processing (such as extrusion blow moulding, blow film extrusion, foaming etc.) is limited by its low melt strength [19,22].

In this context, the present study focuses on the extrusion chemical foaming of PLA. At present only few studies have been reported on the topic. Two commercial PLAs, with different melting temperatures, and an additive combining chemical foaming and nucleating agents incorporated into the PLA at variable amounts, were considered. The effect of these material parameters on cell structure and resulting properties was analysed systematically. For each PLA, the processing conditions (temperature profile, screw speed, die temperature, cooling system) were optimized to obtain a minimum density. The void fraction, cell structure (cell size, cell density, cell-wall thickness) and tensile mechanical properties of materials have been evaluated.

2. Materials and methods

2.1. Materials

Two commercial grades of linear PLA from NatureWorks® LLC, PLA 7000D® and PLA 4032D®, having different melting temperatures were used. The endothermic chemical foaming agent (CFA) which is combined with a nucleating agent was provided by Clariant Masterbatches, under the trademark Hydrocerol® OMAN698483. This is a masterbatch containing sodium bicarbonate and citric acid encapsulated in a PLA matrix. Its gas yield is 55 ml/g (supplier data). The CFA is incorporated into the PLA 7000D® and PLA 4032D® at different weight fractions ranging from 2 to 4 wt%.

2.2. Solution viscometry

Viscosity average molecular weight (M_v) of both PLAs was determined by viscosimetric measurements at 25 °C, in chloroform, using an Ubbelohde capillary viscosimeter (model 0C) according to ISO 1628-1 standard [23]. The equation governing M_v is due to Mark–Houwink–Sakurada. It is a relationship between the intrinsic viscosity $[\eta]$ of the material and M_v (Equation (1)). The intrinsic viscosity $[\eta]$ (Equation (2)) is determined according to the limit value of the reduced viscosity also called viscosity index I (Equation (3)) for an infinite dilution. Three concentrations were used ranging from 0.25 g/dl to 1 g/dl.

$$M_v = \left(\frac{[\eta]}{K}\right)^{\frac{1}{\alpha}} \tag{1}$$

$$[\eta] = \lim_{c \to 0}\left(\frac{\eta - \eta_0}{\eta_0 c}\right) \tag{2}$$

$$I = \frac{\eta - \eta_0}{\eta_0 c} \tag{3}$$

where $K = 4.41.10^{-4}$ dL g^{-1} and $\alpha = 0.72$ are constants depending on the characteristics of the PLA, chloroform and temperature (25 °C) of the solution [6]. η and η_0 represent the viscosity of the polymer solution and the viscosity of the pure solvent respectively. c is the solution concentration (g dL^{-1}).

2.3. Thermal analysis: DSC (differential scanning calorimetry) and TGA (thermogravimetric analysis)

The melting (T_m) and glass transition temperatures (T_g), the degree of crystallinity (χ_c) of PLA have been determined by using DSC. The samples were heated from 20 to 200 °C at a rate of 10 °C/min under nitrogen atmosphere with a Perkin Elmer Pyris Diamond device.

Measuring the melting (ΔH_m) and crystallization (ΔH_c) enthalpies, the degree of crystallinity (χ_c) was calculated by the following equation (Equation (4)).

$$\chi_c = \frac{\Delta H_m - \Delta H_c}{93} \times 100 \tag{4}$$

The constant 93 J/g corresponds to the melting enthalpy of 100% crystalline P(L-LA) or P(D-LA) [1].

The CFA decomposition temperature and the PLA thermal stability were determined by TGA under air, between 20 °C and 700 °C, with a heating rate of 5 °C/min with a Netzsch (STA 409 C) equipment.

2.4. Rheological properties

Dynamic shear rheological measurements were carried out using a rotational rheometer (ARES – TA Instruments) in oscillatory mode. A parallel-plate (25 mm diameter) geometry was selected for the frequency sweeps under controlled strain of 1%. This strain value was first verified to be in the linear viscoelastic region for all the evaluated samples. The angular frequencies were swept from 0.1 to 100 rad s^{-1} at 170 °C with 1.5 mm gap.

2.5. Extrusion and structural analysis of foam

The PLA-based foams were processed using a single-screw extruder (COMPACT - FAIREX Company), equipped with a general-purpose screw (diameter 30 mm, L/D ratio 24). The extrusion is done through a flat die 40 mm width and 1.5 mm gap. Two barrel temperature profiles (A profile and B profile) and three die temperatures with three different screw speeds (10, 20 and 30 rpm) were considered (Table 1). Control samples (neat PLA) are extruded with the C profile (Table 1), because the melting

Table 1
Temperature profiles used for extrusion of neat PLA and PLA/CFA formulations.

Temperature profile	Temperature (°C)					
	Barrel (From hopper to die)					Die
	1	2	3	4	5	6
A	130	150	165	165	170	180–195–210
B	150	170	170	170	180	195
C	170	170	180	180	180	195

temperature of the two PLAs is too high for extrusion with A and B profiles. In this case, the screw speed is 30 rpm. Two cooling systems are used: a slow air cooling, and a faster cooling using a three-roll calendar thermally regulated at 10 °C. Before extrusion, the PLA was dried under vacuum for 15 h at 50 °C. The residual moisture content was about 500 ppm (measured by Karl Fischer method). The various components (PLA and CFA) are dry-mixed before introduction into the hopper of the extruder.

2.5.1. Apparent density

The apparent density (ρ_f) of extruded cellular products is estimated from the weight (m) and the volume (V) of a given sample. Samples were taken from the extruded strips. The sample sizes were measured with a vernier calliper. Their weight (m) is measured using a Mettler AT250 balance with a precision of 0.01 mg. The apparent density (ρ_f), expressed in kg/m^3, is then deducted from Equation (5). The reported values are the average densities measured on 5 samples.

$$\rho_f = \frac{m}{V} \times 10^6 \tag{5}$$

where, m: weight, in grams and V: the geometric volume, in cubic millimetres.

2.5.2. Void fraction

The void fraction (V_f) in % is determined by Equation (6). It is caused by gas (CFA) introduced into the polymer and is quantified by the densities of the extruded neat PLA (ρ_p) and of the PLA foam (ρ_f).

$$V_f = \left(1 - \frac{\rho_f}{\rho_p}\right) \times 100 \tag{6}$$

2.5.3. Cellular structure

The cellular structure was observed using environmental scanning electron microscopy (ESEM) FEI Quanta 200 FEG, with a magnification of 250, under a pressure of 0.83 torr. Other techniques normally used for the analysis of cellular structure are microtomography, ultrasound etc. However, these techniques are either too expensive or of limited precision. Samples were collected from nitrogen quenched extruded parts, perpendicularly to the flow direction. ESEM images, containing approximately 300 cells were then analysed using image processing software (Optimas® 6.5) The cell size distribution was calculated based on the determination of the equivalent diameter (d_i) which is calculated from the area (A_i) of each cell (Equation (7)). However, this value must be corrected in order to limit bias related to the image frame size. This correction is based on the inclusion probability of the cells into the image frame. For this purpose, the methodology of image frame correction, developed by Miles and Lantuejoul [24,25] was applied. The following data were obtained:

(i) The equivalent diameter (based on a circular shape) of the cells d_i (Equation (7))
(ii) The number-average diameter $\overline{d_n}$ (Equation (8)), the size-average diameter $\overline{d_w}$ (Equation (9)) and the polydispersity index (PDI) of the cells diameter distribution (Equation (10)). n_i is the number of cells
(iii) The theoretical cell densities N_c and $N_c^{'}$ (Equations (11) and Equation (12))
(iv) The cell-wall thickness δ (Equation (13))

$$d_i = 2\sqrt{A_i/\pi} \tag{7}$$

$$\overline{d_n} = \frac{\sum(d_i n_i)}{\sum n_i} \tag{8}$$

$$\overline{d_w} = \frac{\sum\left(d_i^2 n_i\right)}{\sum(d_i n_i)} \tag{9}$$

$$\mathrm{PDI} = \frac{\overline{d_i}}{\overline{d_w}} \tag{10}$$

In the case of N_c (Equation (11)) and δ (Equation (13), calculations are based on the assumption that the materials contain only spherical cells [13,14,26–28]. In the case of $N_c^{'}$, calculations are performed assuming that the cells are isotropically distributed. In this case, the square root of the areal cell density of the section is elevated to the cube in order to estimate the volume cell density of the foam [3,29,30]. The latter calculation is based on stereology. It corresponds to the transition from a cell number "n" per unit area "A", to a number of cells per unit volume. According to Gosselin et al. [29], the cells are not truly spherical or isotropic in the case of extrusion and injection foaming because of the deformations involved in the flow direction, due to the shear and elongation stresses. Most realistic models take into account cell deformation in the flow direction, assuming that the cells are ellipsoids of revolution. As a result, several cuts are needed to estimate the three axes of the ellipsoid [29–31]. Therefore, as most authors [13,14,26–28], the simplest model assuming that the cells are perfectly spherical was considered.

$$N_c = \frac{1 - \left(\rho_f/\rho_p\right)}{\left(\pi \overline{d_n}^3/6\right)} \tag{11}$$

$$N_c^{'} = \left(\frac{n}{A}\right)^{3/2} \tag{12}$$

$$\delta = \overline{d_n}\left(\frac{1}{\sqrt{\left(1 - \frac{\rho_f}{\rho_p}\right)}} - 1\right) \tag{13}$$

The measurement uncertainty on the average cell size $\overline{d_n}$, the cell density N_c and the cell-wall thickness δ, is about of 1–7% dependant on the concerned parameter. These values are determined by processing a batch image 3 times. The distribution

of cell size is adjusted by log-normal law according to maximum likelihood estimation.

2.5.4. Open cells content

The open cells content (C_o) of extruded cellular products is quantified using a gas pycnometer (Helium), Micromeritics Accu-Pyc 1330 (Equation (14)). The tests were performed on samples with a dimension of 40 × 30 × 1.50 mm^3. The result is an average value obtained by testing three samples.

$$C_o = \frac{(V_g - V_r)}{V_g} \times 100 \quad (14)$$

where V_g: Geometric volume determined by vernier calliper measurement, and V_r: The actual geometric volume determined by pycnometry.

2.6. Uniaxial tensile properties

The mechanical properties (stress and elongation at yield and break) under tension were measured according to ISO 527-2 [32]. Samples dimensions did not permit to evaluate the Young's modulus. The samples (5A type) were collected from extruded parts, parallel to the extrusion direction, and conditioned at least 3 days at room temperature (23 °C). The tests were performed using a tensile testing machine ZWICK/Z010, equipped with a load cell of 0.5 kN, with a crosshead speed of 2 mm/min. The reported results are an average of 10 samples.

3. Results and discussions

3.1. Characterization of materials prior to extrusion foaming

3.1.1. Melting and glass transition temperatures, degree of crystallinity and viscometric average molecular weight

The melting T_m and glass transition T_g temperatures, the degree of crystallinity χ_c, the viscometric average molecular weight M_v and the density ρ_p (determined on extruded PLA) of both PLAs before extrusion foaming are presented in Table 2.

Only one difference in the melting temperature can be observed. This difference is probably attributed to different optical purities (percentage of D- and L-) of the two PLAs [6]. Indeed, the PLA 7000D® contains 2.7 times more of D-lactic (6.4%) that the PLA 4032D® (2.4%) (value determined by polarimetric analysis).

No difference was observed on the thermal stability of the two PLAs (Fig. 1). Their thermal degradation occurs between 329 °C and 356 °C.

Thermal decomposition of chemical foaming agent (CFA) was observed in the temperature range 152 °C–211 °C with the liberation of CO_2 and H_2O. Decomposition was observed in two stages with a weight loss of 17% (Fig. 1). A residual mass of 23% was observed at the end of the test (700 °C). It is probably due to nucleating agents present in the masterbatch. These results confirm the foaming ability of PLA during extrusion without degradation of the PLA matrix. Indeed, the decomposition of the CFA was observed clearly below the degradation temperature of PLA. This justifies the temperatures choice for foam processing

Table 2
Characteristics of PLA before extrusion chemical foaming.

Polymers	M_v (g/mol)	T_g (°C)	T_m (°C)	χ_c (%)	ρ_p (kg/m^3)
PLA 7000D	90,438	61.4 ± 0.2	152.8 ± 0.7	28.3 ± 0.8	1329 ± 3
PLA 4032D	89,563	68.6 ± 0.7	172.8 ± 1.3	33.5 ± 1.9	1332 ± 11

±: standard deviation.

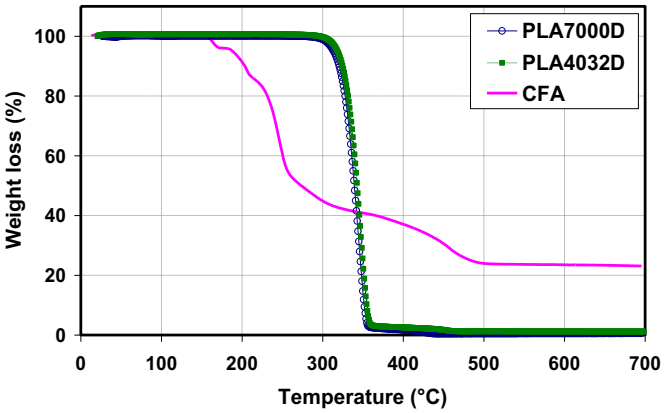

Fig. 1. Thermogravimetric analysis of PLA 7000D®, PLA 4032D® and CFA from 20 °C to 700 °C at 5 °C/min in air.

(Table 1) which ensures the foam build-up (processing above the decomposition temperature of the CFA) while limiting the risk of thermal degradation in the first barrel zones of the extruder (temperature lower than or equal to 170 °C). However, one can anticipate the foaming of PLA 4032D® will be more difficult under the present set of processing conditions (A and B temperature profiles) because its melting (172.8 °C) will occur after the decomposition of CFA and more downstream in the barrel compared to PLA 7000D®. The gas formed in the first barrel zones could be lost before complete melting and pressurization. The gas remaining after melting will be significantly reduced and will have very few time to diffuse in the molten polymer The foaming at the die exit will not be limited.

3.1.2. Rheological properties of PLA

Figs. 2 and 3 show the rheological behaviour of the two PLAs. Fig. 2 shows no difference in viscosity η^* between them. The behaviour of both polymers is quite similar, Newtonian plateau was observed (assuming the Cox-Merz rule checked on the materials under study) at low frequency and a shear thinning effect was seen at higher frequency. The complex viscosity as a function of angular frequency ω is modelled by using Carreau-Yasuda equation (Equation (15)) to determine the Newtonian viscosity η_0 [6,33]. It was observed that η_0 values are 5591 Pa s and 6029 Pa s for PLA 7000D® and PLA 4032D® respectively. Fig. 3 shows that the storage modulus (G') and loss modulus (G'') of both PLAs are the same. The rheological behaviour of a polymer is an important parameter in the

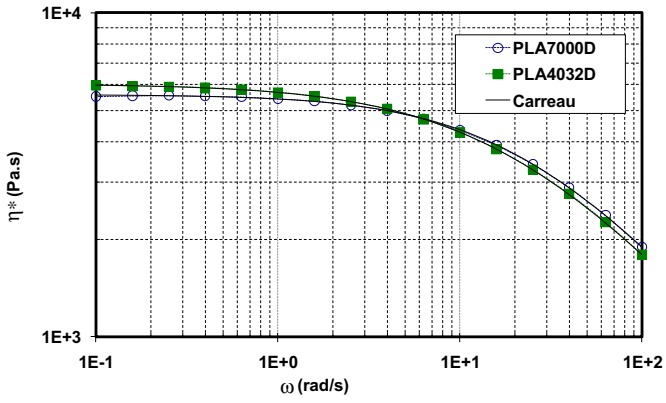

Fig. 2. Complex viscosity (η^*) as a function of angular frequency (ω) for PLA 7000D® and PLA 4032D® at 170 °C, 1% strain and 0.1–100 rad/s.

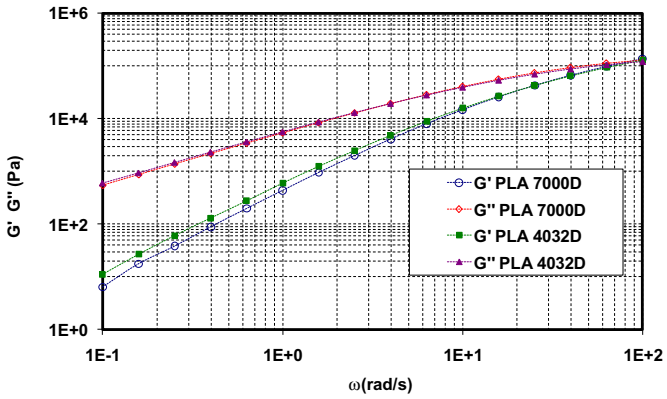

Fig. 3. Storage modulus G' and loss modulus G'' as a function of angular frequency (ω) for PLA 7000D® and PLA 4032D® at 170 °C, 1% strain and 0.1–100 rad/s.

processing of polymeric foams. A slight strain hardening associated to a low viscosity lead to the coalescence and the collapse of the cells resulting in large cells and a low expansion ratio [14,34].

$$\eta(\dot{\gamma}) = \eta_o\left(1 + (\lambda\dot{\gamma})^a\right)^{\frac{m-1}{a}} \quad (15)$$

$\eta(\dot{\gamma})$: viscosity versus shear rate η_0 : Newtonian low shear rate viscosity λ: time constant $\dot{\gamma}$: shear rate m: pseudoplasticity index.

3.2. Optimization of the processing parameters

3.2.1. Influence of the die temperature and the screw speed

For PLA 7000D® with 2 wt% CFA extruded using A temperature profile, at screw speeds of 10 and 30 rpm (which is corresponding to mass flow rates from 1.54 to 2.73 kg/h), the maximum void fraction (Fig. 4) of the extruded product was observed at a die temperature of 195 °C.

Experimental results reported by other researchers [14,35] showed that the foam density gradually decreases (increase in void fraction) with increase in temperature. This increase in temperature promotes the decomposition of CFA, which reduces the foam density to minimum. However, further increase in melting temperature of the polymer leads to increase in the density of the foam due to decrease in viscosity and increase in gas diffusion. This phenomenon can be explained by the competition between two antagonist mechanisms. In fact, an increase in temperature promotes the decomposition of CFA in molten polymer/foaming agent mixture, which accelerates the release of gas. However, the same increase in temperature reduces the viscosity of the molten mixture and favours gas losses by diffusion through the polymer. At low temperatures, the decomposition of the CFA predominates. Conversely, at high temperatures, diffusion phenomena become dominant. The cell walls become weaker with increase in temperature and therefore it is obvious that cell coalescence could occur.

Fig. 4 shows the effect of screw speed on the void fraction of the PLA foam. A maximum void fraction for screw speeds of 10 and 30 rpm was observed at 195 °C. For a screw speed of 20 rpm, the void fraction remains lower than in other cases, and increases gradually with the die temperature until reaching a plateau at around 195 °C. However, the obtained results allow us to define an optimized processing conditions (based on void fraction) i.e. a screw speed of 30 rpm and a die temperature of 195 °C. These processing conditions yielded a maximum void fraction of 42%. Interestingly, these parameters also correspond to maximum production (2.73 kg/h).

3.2.2. Influence of the extrusion temperature profile

Fig. 5 shows the influence of different temperature profiles on the density of PLA 7000D® containing 2 wt% CFA extruded with a screw speed of 30 rpm and a die temperature of 195 °C. The density of the extruded product with the temperature A profile is equal to 766 kg/m^3 (void fraction of 42%), i.e. 14% lower than that of the extruded product with B profile (density of 893 kg/m^3 and void fraction of 33%). It is due to the fact that, temperatures in the first zone of the extruder barrel for B profile are higher than those used for A profile and are equal or higher than onset decomposition temperature of CFA (152 °C). Under these conditions, it is obvious that a premature release of gas, before the complete melting and pressurization of the mixture results in a significant loss of gas useful for foaming. Therefore, the amount of gas available for foaming in successive zones is correspondingly decreased, which leads to a reduction in the void fraction. According to Lee [16], controlling the temperature in the foaming process is an essential step for the processing of foam with a CFA. High temperature in the solid conveying zones (first or second zone) of the extruder leads to a premature release of gas. Indeed, it is likely to observe a lower loss of gas by using the A profile (zones 1 and 2 equal to 130 °C and 150 °C, respectively) compared to B profile, so A profile yielded a higher void fraction (42%) compared to B profile (33%).

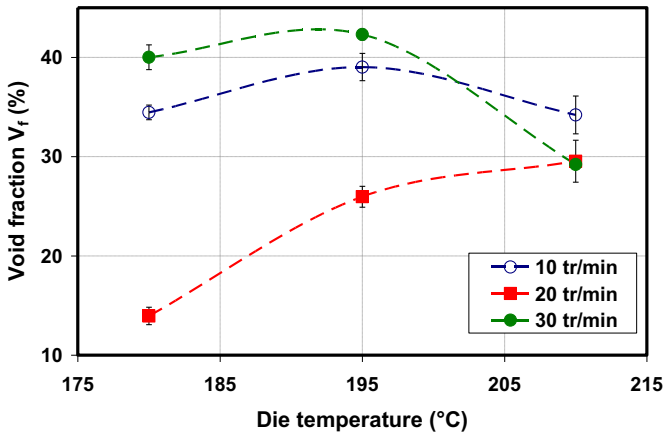

Fig. 4. Evolution of the void fraction in the foams of PLA 7000D® as a function of the die temperature (180 °C; 195 °C and 210 °C) and at different screw speeds (10 rpm, 20 rpm and 30 rpm) – 2 wt% CFA – temperature A profile – slow cooling in air.

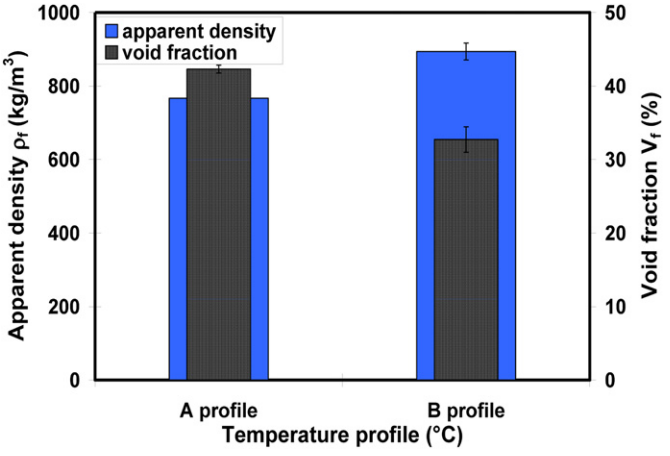

Fig. 5. Evolution of apparent density and void fraction of PLA 7000D® as a function of temperature profile (A profile and B profile) – 2 wt% CFA – die temperature 195 °C and screw speed 30 rpm – slow cooling in air.

3.3. Influence of the cooling system

Fig. 6 compares the cell structures obtained from the foaming of PLA 7000D® (A profile, die temperature 195 °C, screw speed 30 rpm) with an addition of 4 wt% foaming agent with two cooling systems (slow air cooling, fast cooling with a calendar at 10 °C). In the case of slow cooling system, the temperature at the centre of the extruded product is high enough to allow the cell growth progress over a long distance after the die exit. This results in the formation of bigger cells or coalescence of individual cells in the vicinity of the symmetry axis of the strip (Fig. 6a). The use of a faster cooling system in the calendar, constraints the possibility of volume expansion in one direction after die exit and therefore, the central area of the extruded product does not show any large cells (Fig. 6b). The observed results clearly indicate that the cooling system has a significant influence in the processing of cellular materials. Reductions in cell size and cell-wall thickness with an increase in cell density (N_c) were noticed in fast cooling system (Table 3). However, the cell density calculated by extrapolating from 2D to 3D ($N_c^{'}$) remains the same for both cooling systems.

The difference in two cell density values (N_c and $N_c^{'}$) arises from the way cells are indexed, because in a given image all the cells cannot be taken into account. Moreover cells are not perfectly spherical and isotropic. This justifies a little distortion in the value of $N_c^{'}$.

Moreover, the foam skin and core structure obtained with the fast cooling system (Fig. 6b) show the existence of cell-free zones. This is probably due to the increased viscosity of the melt polymer at the exit die and this increase in viscosity hinders the cell growth. These results are in agreement with the results reported in the literature [36].

Fig. 7 shows the distribution of cell size for the foams obtained from PLA 7000D® with both cooling systems. It is clear that the cooling system has no significant effect on the width of the distribution. The polydispersity index (PDI) is similar for both cooling systems. Therefore, in the remaining part of the article, only the air cooling system will be considered.

3.4. Effect of material parameters on the cellular structure and the mechanical properties

3.4.1. Nature of PLA

The nature of the PLA has no significant effect on the void fraction and density of the extruded foam with B profile with a screw speed of 30 rpm (Fig. 8). It was not possible to perform the extrusion foaming of PLA 4032D® with the A profile. In fact, the temperatures in the first two zones of the barrel are too low compared with melting temperature of PLA 4032D® (173 °C). Extrusion foaming caused a locking of the extruder (presence of unmelt polymer).

As reported in the literature [14,16,21,37], the melting and processing temperatures must be taken into account before mixing a polymer with chemical foaming agent (CFA). Finally, one should ensure that CFA should not undergo pre-decomposition or incomplete decomposition during the foaming process. Therefore, the CFA should induce foaming at a temperature between its decomposition temperature and the degradation temperature of the polymer.

Although, the results obtained for both PLAs with respect to their viscometric average molecular weight, shear viscosity and density are similar, only one grade of PLA, i.e. PLA 7000D® was convenient for the production of foam with the chosen CFA. Its melting temperature of about 153 °C, making it able to work at low temperature in the first zones of the extruder barrel, thus avoiding gas loss through the hopper.

3.4.2. Influence of the chemical foaming agent content

3.4.2.1. Void fraction. Irrespective to the PLA nature and/or the temperature profile, the void fraction of the extruded foams gradually increases and thereby decreases in density with increase in the CFA concentration (Fig. 9). This is due to the fact that an increase in foaming agent concentration promotes the release of CO_2 which is thus available for cell growth. In addition, foams containing 2 and 3 wt% of CFA, the void fraction of cellular materials produced from PLA 7000D® with A profile appears to be more effective than those produced with B profile. The void fraction of foams obtained with 4 wt% of CFA is about 47%. Similar results were reported by other authors [38–40] who pointed out that the density of polyolefin and PLA foams was reduced by gradually increasing the amount of foaming agent (between 0.125% and 5% by weight).

Klempner et al. [14] ascertain that the foam density is controlled by the amount of foaming agent. The effectiveness of the foaming agent depends on the polymer and the processing parameters used for foaming (specifically the temperature, because it influences not only the viscosity of the mixture but also the amount of gas evolution during the thermal decomposition of the CFA). This result confirms that the choice of processing parameters could be a compromise between the constraints imposed by the extrusion on one hand and of the foaming on the other hand. In other words, it is necessary that the melting temperature of the polymer remains below the decomposition temperature of the CFA in order to avoid premature decomposition of the foaming agent in the first zones of the extruder barrel. Indeed, the materials obtained with the A profile has a greater void fraction compared to those produced with the B profile.

3.4.2.2. Cellular structure. Table 4 summarizes the structural features of PLA foams, PLA 7000D® extruded with the A profile and PLA 4032D® with the B profile for equivalent die temperature (195 °C) and screw speed (30 rpm). Whatever the material

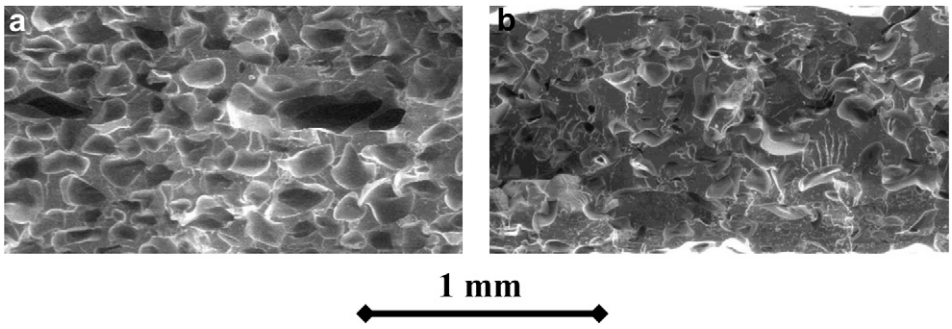

Fig. 6. Cellular structure of PLA 7000D® with 4 wt% of CFA – temperature A profile – die temperature 195 °C – 30 rpm – a) obtained from slow cooling system; b) obtained from fast cooling system.

Table 3
Effect of cooling system (slow and fast) on the cellular structure of PLA 7000D® containing 4 wt% of CFA, extruded with temperature A profile at a die temperature of 195 °C with a screw speed of 30 rpm.

Cooling system	V_f (%)	$\overline{d_n}$ µm	$\overline{d_w}$ µm	PDI	N_c (cells/cm^3) × 10^5	$\dot{N_c}$ (cells/cm^3) × 10^5	δ µm
Slow (in air)	47 ± 1	107 ± 2	122 ± 2	0.88 ± 0.01	7.38 ± 0.51	2.40 ± 0.40	49.26 ± 1
Fast (calendar at 10 °C)	45 ± 1	92 ± 2	105 ± 1	0.88 ± 0.01	10.86 ± 0.75	2.40 ± 0.17	45.59 ± 1

±: standard deviation.

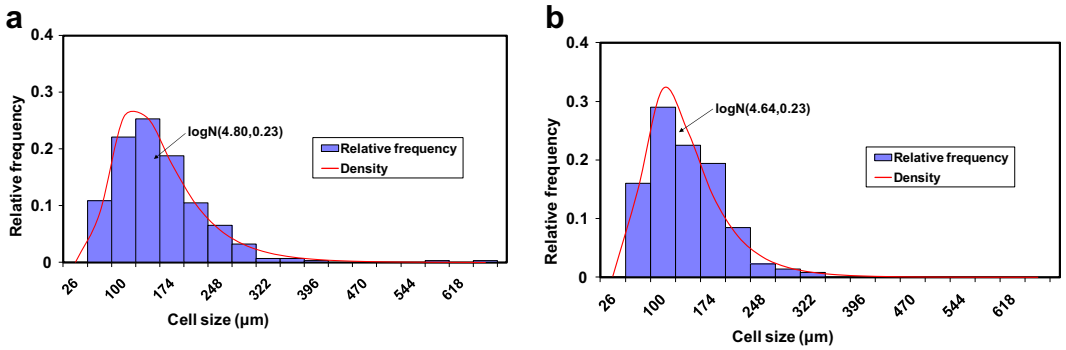

Fig. 7. Effect of different cooling systems (fast and slow) on the distribution of cellular size of PLA 7000D® (4 wt% of CFA; temperature A profile; die temperature 195 °C and screw speed 30 rpm) – a) slow cooling in air b) fast cooling to 10 °C – the parameters of the log-normal log$N(\mu,\sigma^2)$ density function are μ (mean) and σ^2 (variance).

considered, the resulting foam structure is relatively homogeneous (polydispersity index PDI close to 1). It can also be noticed that, in all cases, the open cells content (C_o) is low (compared to flexible foams used for soundproofing, for example where the content of open cells is about 90%), less than 27%. Thus, PLA foams have large amounts of closed cells as it is the case for extruded polyolefin foams (PP, PE, etc.) and for PLA foams produced in an autoclave under pressure [14,20,26].

The influence of CFA content on open cells content is similar for both PLA matrices. Indeed, an increase of 2–4 wt% of CFA content increases the open cells content from 10 to 19% and from 19% to 26% for PLA 7000D® and PLA 4032D® respectively. Nevertheless, open cells content is greater in the case of PLA 4032D®. This is related with the very high temperature profile (B profile) used which yields not only a high gas formation but also decreases the viscosity of the mixture. According to Klempner et al. [14], during the initial growth these cells are closed. However, they become open when one or more cell wall breaks. This is usually due to excessive thinness of the walls which are not rigid enough to withstand the internal pressure of the cell. This phenomenon is thus linked to the low viscosity of the system. As a result, an increase in the amount of CFA from 2 to 4 wt% leads to an automatic reduction in the viscosity of the mixture causing increased open cells content. The decomposition of CFA in water and in carbon dioxide or nitrogen added to the polymer which encapsulates the CFA contributes to the plasticization of the polymer [16]. Besides, in molten state, the decomposition products of the foaming agent act as plasticizers. This allows for example reducing the cycle time production of a part [41].

An increase in CFA content between 2 and 4 wt% induces an increase in cell size (around 16%). However, the cell-wall thickness (δ) remains virtually unchanged (between 46 and 49 µm) for materials based on PLA 7000D® extruded with A profile (Table 4 and Fig. 10). In the present study, the increase in cell size observed for the PLA 7000D®, leads to a decrease in cell density

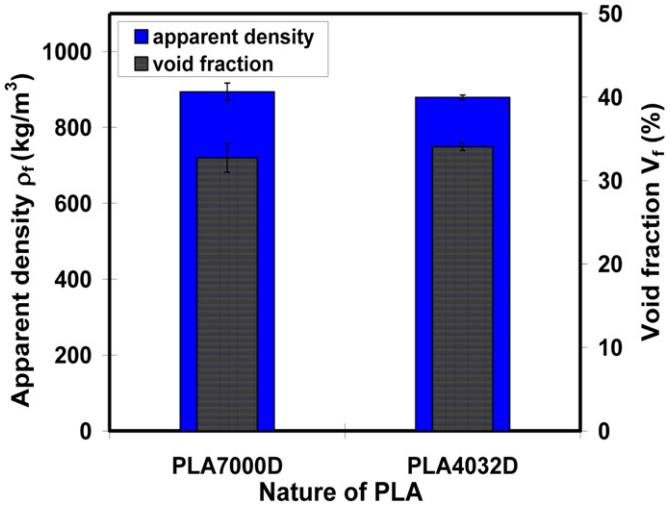

Fig. 8. Evolution of apparent density and void fraction with respect to nature of PLA (PLA 7000D® and PLA 4032D®) for 2 wt% CFA – B profile; die temperature 195 °C – 30 rpm – slow cooling.

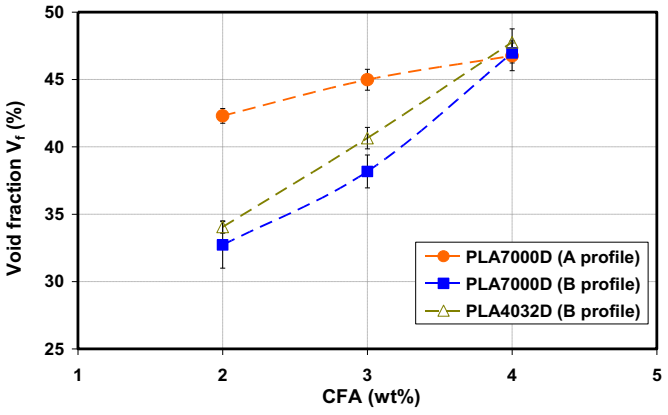

Fig. 9. Evolution of void fraction as a function of foaming agent content (CFA) for PLA 7000D® and PLA 4032D® with A profile and B profile; die temperature 195 °C, screw speed 30 rpm – slow air cooling.

Table 4
Cell size (d_n) and density (N_c and $N_c^{'}$), polydispersity index of cell size (PDI), cell-wall thickness (δ) and open cell content (C_o) as a function of CFA content (2, 3 and 4 wt %) – PLA 7000D® A profile and PLA 4032D® B profile; screw speed 30 rpm; die temperature 195 °C – slow cooling.

Polymers	CFA (%)	$\overline{d_n}$ (μm)	$\overline{d_w}$ (μm)	PDI	N_c (cells/cm^3) × 10^5	$N_c^{'}$ (cells/cm^3) × 10^5	δ (μm)	C_o (%)
PLA7000D	2	90 ± 2	105 ± 1	0.86 ± 0.01	11.25 ± 0.78	3.48 ± 0.8	48 ± 1	10.9 ± 0.2
	3	95 ± 2	104 ± 1	0.91 ± 0.01	10.13 ± 0.70	3.00 ± 0.30	46 ± 1	14.7 ± 1.1
	4	107 ± 2	122 ± 2	0.88 ± 0.01	7.38 ± 0.51	2.40 ± 0.40	49 ± 1	19.2 ± 0.7
PLA4032D	2	134 ± 3	144 ± 2	0.93 ± 0.01	2.72 ± 0.19	0.77 ± 0.05	95 ± 2	19.1 ± 1.5
	3	125 ± 3	174 ± 2	0.72 ± 0.01	4.02 ± 0.28	0.89 ± 0.30	71 ± 1	24.5 ± 1.3
	4	130 ± 3	152 ± 2	0.86 ± 0.01	4.19 ± 0.29	1.46 ± 0.30	58 ± 1	26.76 ± 1.1

±: standard deviation.

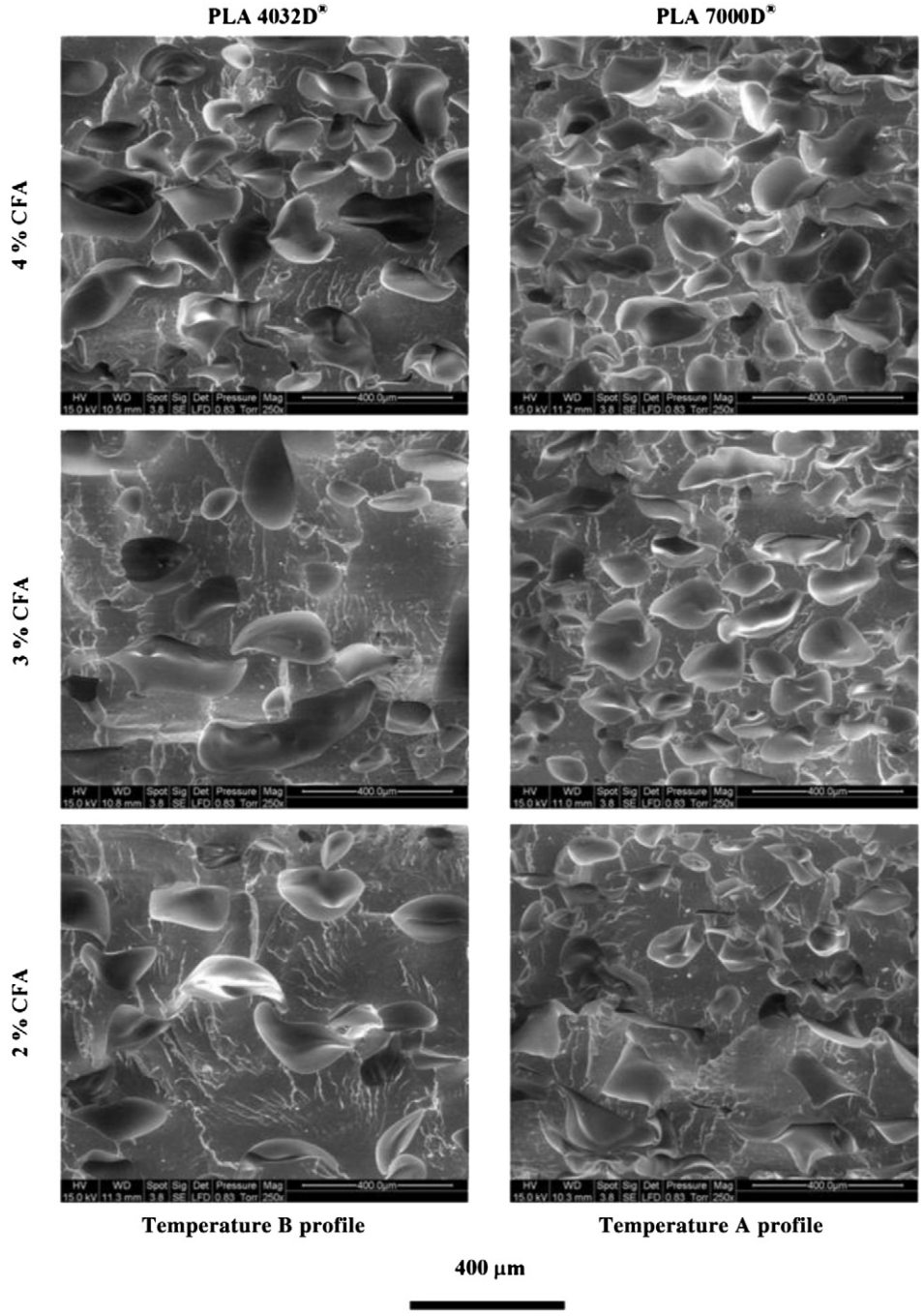

Fig. 10. Cellular structure of PLA 7000D® (A profile) and PLA 4032D® (B profile) as a function of CFA content (2, 3 and 4 wt%) – die temperature 195 °C – screw speed 30 rpm – slow cooling.

regardless of the equation used (Equation (11) or Equation (12)). This could be explained by the increase in the amount of gas available for cell growth. These results explain in the same manner the increase in void fraction (Fig. 10) of cellular materials by increasing the amount of CFA. Because the number of nucleated cells and their growth which control the void fraction of the materials during the foaming process, are highly dependant on the amount of gas molecules dissolved in the molten polymer matrix [42,43].

PLA 4032D® has a different behaviour. The average diameter ($\overline{d_n}$) of cells becomes minimum at an intermediate CFA content. This behaviour may be related to the mechanism of cell growth which is heavily dependant on viscoelastic properties of the polymer during the foaming process. Indeed, the PLA 4032D® is extruded with a high temperature profile (B profile) compared to PLA 7000D® (A profile), also CFA acts as a plasticizer, implying a decrease in the viscosity of mixture. This is consistent with a decrease in the cell size correlated with an increase of the amount of CFA from 2 to 3 wt%. Beyond 3 wt%, an increase in the amount of CFA increases cell size, because not only the viscosity of the mixture decreases, but also there is no more gas available for cell growth. However, the cell density (N_c) increases and the cell-wall thickness (δ) decreases with an increase of CFA content. This is related to a reduction of the cell size up to 3 wt% of CFA; beyond, the CFA content (in the studied range) influences just a little the cell density.

Figs. 11 and 12 show the distribution of cell size as a function of CFA content. The distribution of cell size is almost identical for the three materials based on PLA 7000D (containing 2, 3 and 4 wt% of CFA). For this PLA grade, the number of big cells (>322 μm) is very low (<3%) whatever the CFA content.

The effect of CFA content is more significant for the materials based on PLA 4032D (Fig. 12). In this case the width of the cell size distribution (variance of the log-normal density function) increases unmonotonously with the CFA content. The increase in CFA content from 2 to 3 wt% leads to an increase in small and big cells. More small cells are formed because more gas is generated during the extrusion process and higher content of nucleating particles is available in the polymer while foaming. Big cells are formed because of the cell coalescence mechanism.

The PLA 7000D® extruded foams with the A profile have a cell density very significantly greater than PLA 4032D® extruded foams with the B profile (Table 4 and Fig. 10). This may be due to the quality of the mixing in the extruder. As the melting temperature of PLA 4032D® is 173 °C, it is likely that the homogeneity of the mixing PLA 4032D®/CFA is insufficient. Or, any gas loss in the first zones of the extruder barrel induced by high temperatures could lead to areas devoid of cells (Fig. 10).

An overall result indicates that PLA 7000D® is the most suitable for the production of foam by extrusion using chemical foaming agent. Indeed, its melt temperature (153 °C) is compatible with the initial decomposition temperature of the foaming agent used (152 °C), which allows to limit the gas loss in the extruder (A profile).

However, it was observed that the average cell size and the cell density obtained in the present study are comparable to those of conventional foams (non microcellular) (12–120 μm for the average cell size and 10^2 to 10^6 cells/cm^3 for the cell density) [14,16]. In contrast, the cell size is significantly higher than the reported values by other researchers [17,20,27,44] for microcellular PLA foams. But, the foaming process they used was different (in an autoclave under pressure with saturated CO_2) and PLA are often filled with nanofillers or modified by chain-extenders.

3.4.3. *Mechanical properties of materials*

Table 5 represents the mechanical properties of foams with different grades of PLA. It was observed that, whatever the PLA nature, an increased addition of foaming agent reduces the yield stress and stress at break under tension (Table 5). This is due to the fact that addition of CFA increases the void fraction (thereby reduces the effective bulk cross section of the sample due to the formation of cellular structure) and increased number of cells acts

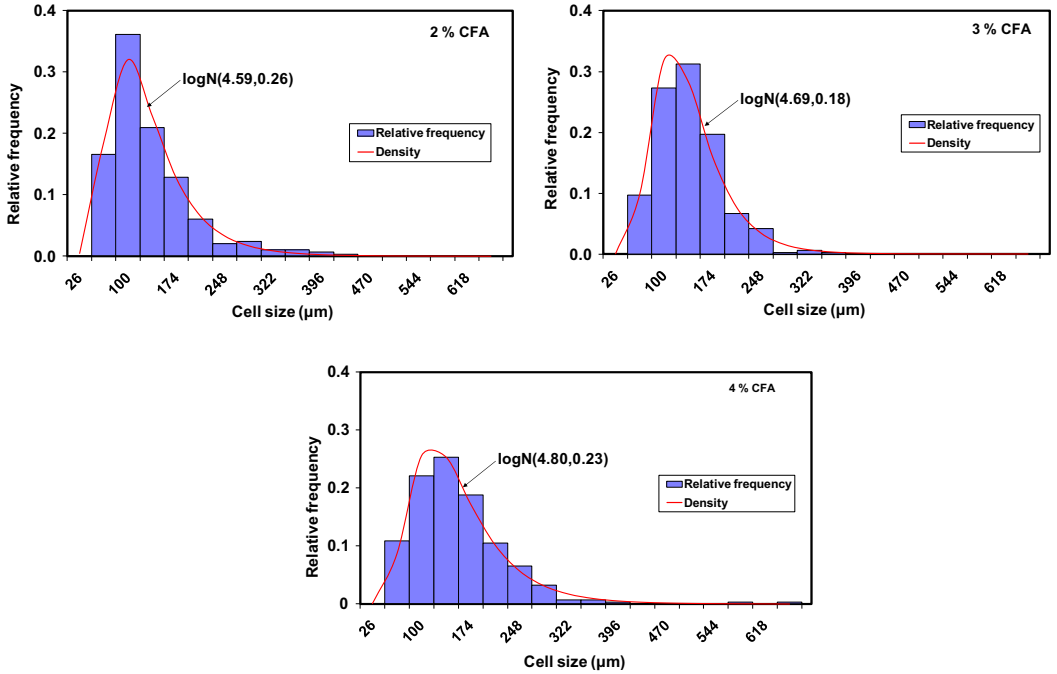

Fig. 11. Distribution of cell size as a function of CFA content (2, 3 and 4 wt%) for PLA 7000D® – A profile; die temperature 195 °C – screw speed 30 rpm - slow cooling – the parameters of the log-normal log$N(\mu,\sigma^2)$ density function are μ (mean) and σ^2 (variance).

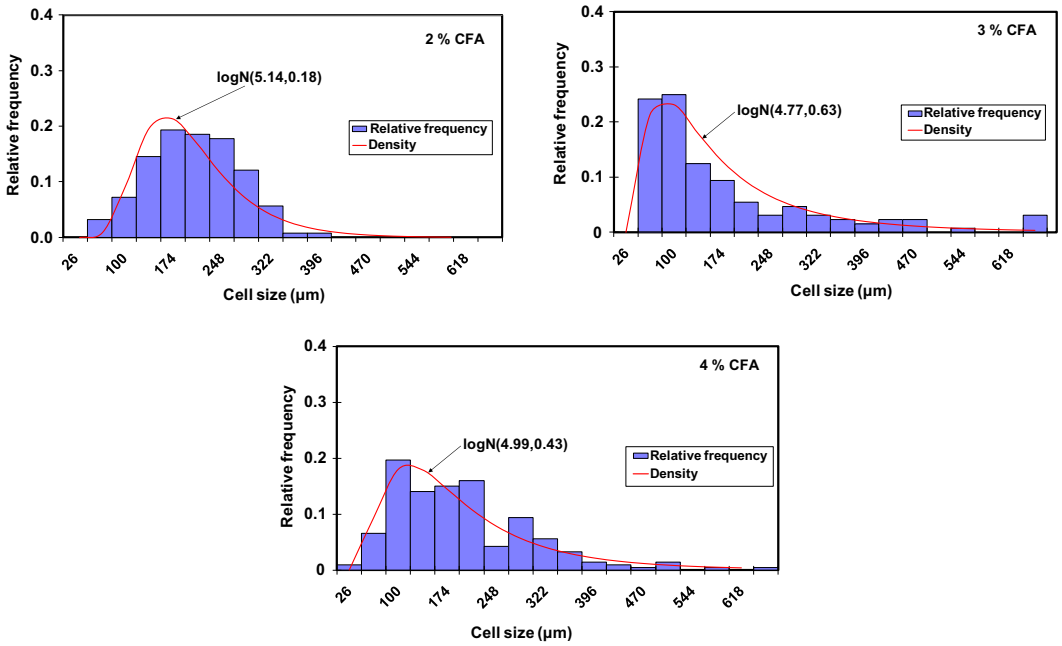

Fig. 12. Distribution of cell size as a function of CFA content (2, 3 and 4 wt%) for PLA 4032D® – B profile; die temperature 195 °C – screw speed 30 rpm – slow cooling – the parameters of the log-normal log$N(\mu,\sigma^2)$ density function are μ (mean) and σ^2 (variance).

Table 5
Tensile properties as a function of CFA concentration (2, 3 and 4 wt%) for PLA 7000D® (A profile) and PLA 4032D® (B profile) – die temperature 195 °C – screw speed 30 rpm – slow cooling (σ_y: yield stress, ε_y: elongation at yield stress, σ_r: stress at break, ε_r: elongation at break).

Polymer	CFA1 (%)	V_f (%)	σ_y (MPa)	ε_y (%)	σ_r (MPa)	ε_r (%)
PLA 7000D®	0	–	60.51 ± 1.58	10.33 ± 0.94	57.34 ± 1.36	11.12 ± 0.86
	2	42 ± 1	36.00 ± 2.84	8.41 ± 0.32	33.38 ± 2.18	9.95 ± 0.71
	3	45 ± 1	25.65 ± 1.33	8.84 ± 0.39	21.51 ± 1.72	11.59 ± 0.92
	4	47 ± 1	23.71 ± 0.90	8.37 ± 0.55	20.49 ± 1.08	10.28 ± 1.16
PLA 4032D®	0	–	59.51 ± 2.26	9.40 ± 0.42	54.61 ± 4.99	10.19 ± 0.61
	2	34 ± 1	40.54 ± 3.27	10.24 ± 0.89	37.91 ± 3.90	11.51 ± 1.23
	3	41 ± 1	30.68 ± 2.40	8.61 ± 0.70	27.14 ± 3.44	10.43 ± 1.11
	4	48 ± 1	26.77 ± 1.24	9.44 ± 1.36	22.87 ± 1.12	11.50 ± 1.60

as sites for damage (especially small cells induce stress concentrations). In contrast, the elongation at yield and break of the foams are low and independent of the CFA content. Similar results were reported for PVC and PUR foams [12,45].

The specific mechanical properties of all samples are also detailed in Table 6. Indeed, to follow the evolution of the properties/weight ratio (called specific stress) of various materials carried out, we used the concept of performance index [46]. A significant reduction in specific mechanical properties was observed after foaming as compared to solid materials (Table 5). However, the specific yield stress and stress at break for cellular materials with 2 wt% CFA showed no difference from those of solid materials, which implies that the properties/weight ratio is not compromised by the foaming of PLA up to 2 wt% CFA. Beyond this amount, specific properties significantly decrease. Fig. 13 shows that PLAs and PLAs based foam containing 2 wt% of CFA are most powerful in term of yield stress (specific yield stress highest) and located on the same line of performance.

Table 6
Specific tensile properties as a function of CFA concentration (2, 3 and 4 wt%) for PLA 7000D® (A profile) and PLA 4032D® (B profile) – die temperature 195 °C – screw speed 30 rpm – slow cooling (σ_y/ρ: specific yield stress, σ_r/ρ: specific stress at break).

Polymers	CFA (%)	V_f (%)	σ_y/ρ ($\times 10^3$ Pa m^3 kg^{-1})	σ_r/ρ ($\times 10^3$ Pa m^3 kg^{-1})
PLA7000D®	0	–	45.53 ± 1.19	43.15 ± 1.36
	2	42 ± 1	46.94 ± 3.70	43.52 ± 2.18
	3	45 ± 1	35.09 ± 1.82	29.43 ± 1.72
	4	47 ± 1	33.54 ± 1.27	28.98 ± 1.08
PLA 4032D®	0	–	44.68 ± 1.70	41.00 ± 4.99
	2	34 ± 1	46.12 ± 3.72	43.13 ± 3.90
	3	41 ± 1	38.79 ± 3.03	34.31 ± 3.44
	4	48 ± 1	38.46 ± 1.78	32.86 ± 1.12

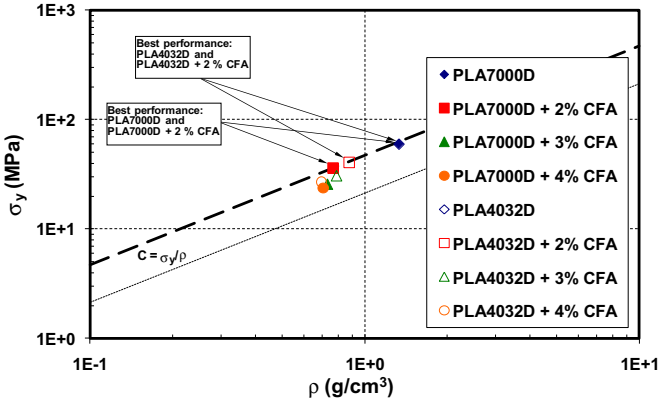

Fig. 13. Yield stress (σ_y) tensile properties as a function of density (ρ) to various contain of CFA in log–log representation (—— guiding line of C constant; – – – guiding line which is by the top to experimental points).

4. Conclusions

Foaming of two commercial grades of PLA (PLA 7000D® and PLA 4032D®) was performed through single-screw extrusion by the incorporation of an endothermic chemical foaming agent (CFA). For each PLA, a set of processing parameters (screw speed, die temperature, temperature profile and cooling system) has been optimized to reduce the density of the final product. However, even in these optimized processing conditions, PLA 4032D® foaming remained difficult. Its melting temperature is higher than the onset decomposition temperature of the chemical foaming agent. That induces a significant gas loss through the hopper (before complete melting and pressurization of the mixture) and thus reduces the efficiency of the foaming agent.

In the case of PLA 7000D®, density reduction (maximal 47% of void fraction obtained with addition of 4 wt% of CFA) is due to an intermediate die temperature (195 °C) to achieve a balance between the different times available for cell growth and diffusion of released gases of the foaming agent, through the molten polymer. Moreover it was shown that the use of a calendar cooling system may limit the formation of large cells (107 μm–92 μm) in the central area of the profile, without reducing the void fraction (further works showed the same conclusion for 2 and 3 wt% of CFA).

For optimized processing conditions, a homogeneous cell structure (polydispersity index close to 1) was obtained whatever the grade of PLA, as well as low open cells contents (27%) compared to more conventional foams. For PLA 7000D®, the increase in CFA content (2 wt% to 4 wt%) decreases the cell density ($11.25.10^5$ cells/cm^3–$7.38.10^5$ cells/cm^3) and increases the cell size (90 μm–107 μm). Conversely, for PLA 4032D®, an increase in cell density ($2.72.10^5$ cells/cm^3–4.19 cells/cm^3) and a decrease in cell-wall thickness (95 μm–58 μm) were observed. Decrease in yield stress and stress at break was also observed with the increase in CFA content, however it has no significant effect on the elongation at break. On the other hand, the specific yield stress (approximately 46.10^3 Pa m^3 kg^{-1}) for cellular materials with 2 wt% CFA showed no difference from those of solid materials.

References

[1] Martin O, Avérous L. Polymer 2001;42:6209–19.
[2] Nugroho P, Mitomo H, Yoshii F, Kume T. Polym Degrad Stab 2001;72:337–43.
[3] Pilla S, Kramschuster A, Yang L, Lee J, Gong S, Turng LS. Mat Sci Eng C 2009;29:1258–66.
[4] Chandra R, Rustgi R. Prog Polym Sci 1998;23:1273–335.
[5] Matuana LM. Bioresour Technol 2008;99:3643–50.
[6] Lim LT, Auras R, Rubino M. Prog Polym Sci 2008;32:820–52.
[7] Bastioli C. Handbook of biodégradable polymers. Smithers Rapra Technology; 2005.
[8] Bleach NC, Nazhat SN, Tanner KE, Kellomaki M, Tormala P. Biomaterials 2002;23:1579–85.
[9] Kale G, Auras R, Singh SP. Packag Technol Sci 2007;20:49–70.
[10] Graupner N, Herrmann AS, Müssig J. Compos Part A 2009;40:810–21.
[11] Fink HP, Ganster J. Macromol Symp 2006;244:107–18.
[12] Kabir MdE, Saha MC, Jeelani S. Mat Sci Eng A 2006;429:225–35.
[13] Tsivintzelis I, Pavlidou E, Panayiotou C. J Supercrit Fluid 2007;42:265–72.
[14] Klempner D, Sendijarevic V. Handbook of polymeric foams and foam technology. 2nd ed. Munich: Carl Hanser Verlag; 2004.
[15] Innovation 128. Les matériaux en mousse et leurs applications industrielles. Innovation 128, Tech Tendances; 1998.
[16] Lee ST. Foam extrusion: principles and practice. Lancaster, USA: Technomic Publishing Company; 2000.
[17] Tsivintzelis I, Angelopoulou AG, Panayiotou C. Polymer 2007;48:5928–39.
[18] Chen G, Ushida T, Tateishi T. Biomaterials 2001;22:2563–7.
[19] Di Y, Iannace S, Di Maio E, Nicolais L. J Polym Sci Pol Phys 2005;43:689–98.
[20] Ray SS, Okamoto M. Macromol Rapid Comm 2003;24:815–40.
[21] Greco A, Maffezzoli A, Manni O. Polym Degrad Stab 2005;90:256–63.
[22] Pagnoulle C, Stassin F, Chapelle G, Jerome R. Method for preparing biodegradable polyester foams, polyester foams obtained thereby, and the use thereof, Belgium, WIPO Patent Application WO/2004/108806, 2004.
[23] International Organization for Standardization, ISO 1628-1:2009; 2008.
[24] Coster M, Chermant JL. Précis d'analyse d'images. Paris: Centre National de la Recherche Scientifique; 1989.
[25] Avérous L, Quantin JC, Lafon D, Crespy A. Int J Polym Anal 1995;1:339–47.
[26] Alavi SH, Gogoi BK, Khan M, Bowman BJ, Rizvi SSH. Food Res Int 1999;32:107–18.
[27] Ema Y, Ikea M, Okamoto M. Polymer 2006;47:5350–9.
[28] Gendron R. Thermoplastic foam processing: principles and development. CRC Press; 2004.
[29] Gosselin R, Rodrigue D. Polym Test 2005;24:1027–35.
[30] Vázquez MO, Ramírez-Arreola DE, Bernache J, Gómez C, Robledo-Ortiz JR, Rodrigue D, et al. Macromol Symp 2009;283–284:152–8.
[31] Zepeda Sahagún C, González-Núñez R, Rodrigue D. J Cell Plast 2006;42:469–85.
[32] International Organization for Standardization, ISO 527–532:1996, ed. AFNOR, 1996.
[33] Dorgan JR, Lehermeier H, Mang M. J Polym Environ 2000;8:1–9.
[34] Petra P, Beate K, Jens S, Helmut M. Macromol Symp 2007;245:400–8.
[35] Park CB, Behravesh AH, Venter RD. Polym Eng Sci 1998;38:1812–23.
[36] Sauceau M, Nikitine C, Rodier E, Fages J. J Supercrit Fluid 2007;43:367–73.
[37] Bledzki AK, Faruk O. Compos Part A Appl S 2006;37:1358–67.
[38] Lee CH, Lee KJ, Jeong HG, Kim SW. Adv Polym Tech 2000;19:97–112.
[39] Lee ST, Kareko L, Jun J. J Cell Plast 2008;44:293–305.
[40] Matuana LM, Faruk O, Diaz CA. Bioresour Technol 2009;100:5947–54.
[41] Markarian J. Plast Addit and Compd 2006;8:22–5.
[42] Baldwin DF, Park CB, Suh NP. Polym Eng Sci 1996;36:1446–53.
[43] Matuana LM, Park CB, Balatinecz JJ. Polym Eng Sci 1997;37:1137–47.
[44] Di Y, Iannace S, Di Maio E, Nicolais L. Macromol Mater Eng 2005;290:1083–90.
[45] Lin HR. Polym Test 1997;16:429–43.
[46] Ashby MF. Materials selection in mechanical design. 2nd ed. Oxford: Butterworth-Heinemann; 1999.